Cardiomyocyte differentiation of bone marrow-derived Oct-4$^+$CXCR4$^+$SSEA-1$^+$ very small embryonic-like stem cells

WOJCIECH WOJAKOWSKI[1], MICHAL TENDERA[1], MAGDA KUCIA[2], EWA ZUBA-SURMA[2,3], KRZYSZTOF MILEWSKI[4], DAVID WALLACE-BRADLEY[4], MACIEJ KAZMIERSKI[1], PAWEL BUSZMAN[1], EUGENIUSZ HRYCEK[1], WIESLAW CYBULSKI[1], GRZEGORZ KALUZA[4], PIOTR WIECZOREK[1], JANINA RATAJCZAK[2] and MARIUSZ Z. RATAJCZAK[2]

[1]Third Division of Cardiology, Medical University of Silesia, Katowice, Poland; [2]Stem Cell Institute at James Graham Brown Cancer Center, University of Louisville, Louisville, KY, USA; [3]Department of Medical Biotechnology, Jagiellonian University, Kraków, Poland; [4]Cardiovascular Research Foundation, Orangeburg, NY, USA

Received March 1, 2010; Accepted April 16, 2010

DOI: 10.3892/ijo_00000671

Abstract. VSELs are a population of rare Oct-4$^+$CXCR4$^+$ CD133$^+$lin$^-$CD45$^-$ cells that are deposited during early embryogenesis in developing organs/tissues as a reserve population of pluripotent stem cells for regeneration. We reported recently that they are mobilized into peripheral blood during acute myocardial infarction (AMI) in mice and humans. However, although freshly isolated VSELs in experimental AMI mouse models improve cardiac function, the number of these cells is limited and an *ex vivo* expansion strategy is needed to employ these cells more efficiently for cardiac regeneration. The aim of this study was to establish an efficient method to expand *ex vivo* BM-derived very small embryonic-like stem cells (VSELs) into cardiomyocytes. VSELs, highly purified by FACS from the bone marrow of GFP transgenic mice, were expanded over C2C12 cell line myoblasts and exposed to cardiac differentiating media. The changes in gene expression during cardiac differentiation of VSELs were evaluated by RTQ-PCR, immunostaining and gene array analysis. We developed an efficient, two-step, *ex vivo* expansion/differentiation model of BM-derived VSELs into cardiomyocytes. First, purified GFP$^+$ VSELs are plated over C2C12 murine cell line myoblasts, where they expand and differentiate into characteristic spheres. Subsequently, cells from these spheres are expanded on cardiac differentiating media into cardiomyocytes. This study demonstrates that murine BM-derived VSELs can be efficiently expanded *in vitro* and differentiated into cardiomyocytes.

Correspondence to: Professor Mariusz Z. Ratajczak, Stem Cell Institute, University of Louisville, 500 South Floyd Street, Louisville, KY 40202, USA
E-mail: mzrata01@louisville.edu

Key words: very small embryonic-like cells, bone marrow, cardiomyocyte

Introduction

Adult bone marrow (BM), in addition to hematopoietic stem cells (HSCs), contains a population of rare cells which may participate in cardiac and endothelial repair (1). These cells are heterogeneous and include endothelial progenitor cells (EPCs), multipotent mesenchymal stromal cells (MSCs) as well as cells expressing several markers typical for pluripotent stem cells (PSCs), such as Oct-4, Nanog and SSEA-1. These adult-BM-derived PSCs may be of particular interest because of their ability to differentiate into cells from all three germ layers, including cardiac myocytes and vascular endothelial cells. These cells were named very small embryonic-like stem cells (VSELs) and are purified from adult BM, peripheral blood (PB) and umbilical cord blood (UCB) using a multiparameter live cell sorting technique based on i) their small size, ii) the expression of stem cell markers (CXCR4 and CD133 in humans and Sca-1 in mice) and iii) the absence of hematopoietic antigen CD45 and lineage markers (CD45$^-$Lin$^-$ cells) (2,3). Experimental studies in murine models of acute myocardial infarction (AMI) demonstrated that this rare population of cells is also enriched in early markers of cardiac and endothelial lineages (GATA-4, Nkx2.5/Csx, VE-cadherin, von Willebrand factor). VSELs migrated to stromal-derived factor-1 (SDF-1) gradient and underwent rapid mobilization into peripheral blood in experimental AMI mouse models (4,5). In addition to BM, VSELs were also identified in several murine solid organs including the heart and brain, as well as in umbilical cord blood and peripheral blood in adult humans (3,5). We envision that VSELs are quiescent progeny of epiblast-derived PSCs that are deposited during organogenesis in developing organs (6,7). In experimental AMI mouse models the intramyocardial injection of VSELs was more efficient than that of HSCs and placebo at improving global and regional left ventricular contractility, as well as reducing myocardial hypertrophy. This effect was demonstrated using a small total number of VSELs (10,000 cells), while a much higher number of HSCs (100,000 cells) was not effective (8). Recently, we demonstrated the mobilization of VSELs expressing PSC, early

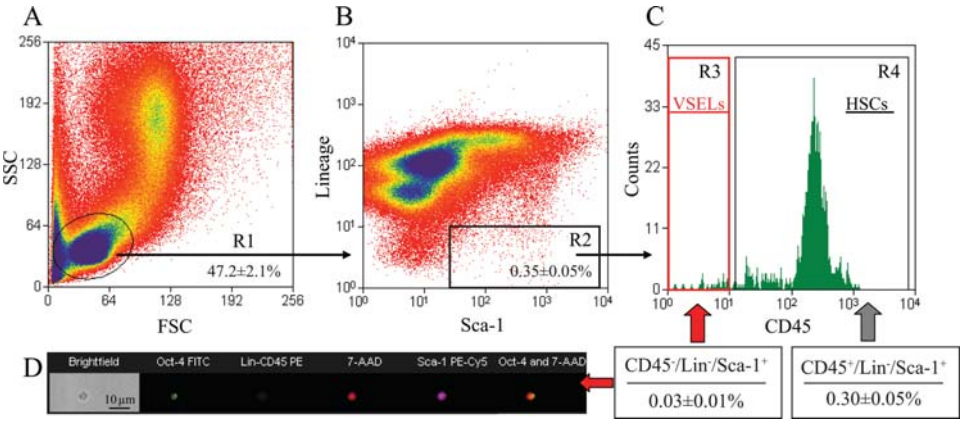

Figure 1. Gating strategy for sorting VSELs by FACS. BM-derived VSELs were isolated from immunofluorescence-stained murine BM-nucleated cells by FACS. Agranular, small BM cells were visualized by dot plots showing forward scatter (FSC) vs. side scatter (SSC) signals, which are related to the size and granularity/complexity of the cell, respectively (panel A). Cells from region R1 were further analyzed for Sca-1 and Lin expression and only Sca-1$^+$/Lin$^-$ events were included in region R2 (panel B). The region R2 population was subsequently sorted based on CD45 marker expression into CD45$^-$ and CD45$^+$ subpopulations and visualized by histogram (panel C, regions R3 and R4, respectively). CD45$^-$/Lin$^-$/Sca-1$^+$ cells (VSELs) were sorted as events enclosed in logical gates, including regions R1, R2 and R3, while CD45$^+$/Lin$^-$/Sca-1$^+$ cells (HSCs) from gates including regions R1, R2 and R4. Percentages of the average content of each cellular subpopulation (mean ± SD) in fully BM nucleated cells are shown. The representative image of freshly sorted Oct-4$^+$ VSEL obtained by the ImageStream system is shown (panel D). Oct-4 staining is shown in green (FITC).

cardiac and endothelial markers in patients with acute MI (9). This suggests that BM-derived VSELs can participate in myocardial repair and that their potential for cardiogenic differentiation should be further investigated.

In the present study, by employing a two-step expansion model, we provide evidence that BM-derived VSELs can be expanded *ex vivo* into cardiomyocytes. In the first step, VSELs are plated in co-cultures with C2C12 myoblasts where they form characteristic spheres. Subsequently, cells isolated from these spheres are plated on cardiac differentiation media to expand them into maturing cardiomyocytes. Finally, we characterized this phenomenon by employing gene array analysis.

Materials and methods

Animals. Pathogen-free, 4-8-week old female wild-type C57BL/6 and green fluorescent protein transgenic C57BL/6-Tg(ACTB-EGFP)1Osb/J mice (The Jackson Laboratory, Bar Harbor, ME, USA) were used. The present study was performed in accordance with the guidelines stipulated by the Animal Care and Use Committee of the University of Louisville School of Medicine and the Guide for the Care and Use of Laboratory Animals [Department of Health and Human Services, Publication No. (NIH 86-23)].

Bone marrow harvesting and live-cell sorting of VSELs. Fig. 1 illustrates the protocol for the isolation, sorting and analysis of VSELs from murine BM samples. BM was flushed with RPMI-1640 media (Gibco, Invitrogen) from the femurs and nucleated cells were isolated by lysis of erythrocytes with lysing buffer (1X PharmLyse; BD Biosciences, San Jose, CA, USA) in room temperature for 15 min and subsequently washed twice in RPMI-1640 media. Cells were resuspended in RPMI-1640 media with 2% heat-inactivated fetal bovine serum (FBS; Gibco, Invitrogen) for immunolabeling. For sorting, cells were stained with the following rat anti-mouse antibodies: anti-Ly-6A/E (Sca-1)-biotin (clone E13-161.7), anti-CD45-APC-Cy7 (clone 30-F11) and anti-hematopoietic lineages markers (Lin). The anti-Lin cocktail includes the following antibodies: anti-CD45R/B220-PE (clone RA3-6B2), anti-Gr-1-PE (clone RB6-8C5), anti-TCRαß PE (clone H57-597), anti-TCRγδ PE (clone GL3), anti-CD11b PE (clone M1/70) and anti-Ter-119 PE (clone TER-119). All antibodies, as well as streptavidin-PE-Cy5 (for secondary Sca-1 staining) were added at saturating concentrations. Cells were incubated on ice for 30 min, then washed and resuspended for sorting in CSM at concentrations of 5-10x10^6 cells/ml. Cells were sorted using a multiparameter, live sterile cell sorting system (MoFlo, Beckman Coulter, Fullerton, CA, USA) according to previously published protocols, and were used for real-time RT-PCR, immunochemistry, ImageStream analysis and cardiogenic differentiation (2).

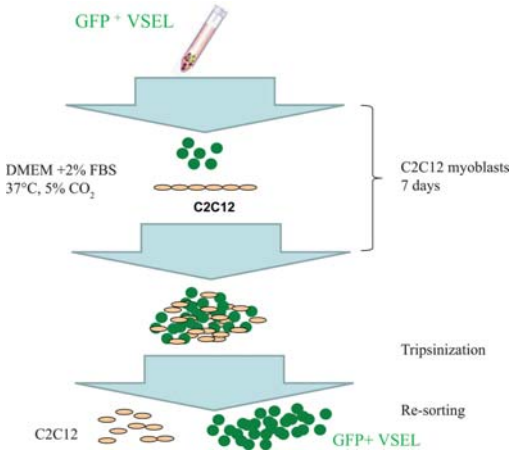

Figure 2. *In vitro* expansion of freshly sorted VSELs. VSELs were plated over the feeder layer of C2C12 murine myoblasts and, after 7 days of coculture, formed sphere-like clusters (VSEL-DSs). E-GFP$^+$ VSELs were separated from myoblasts by FACS.

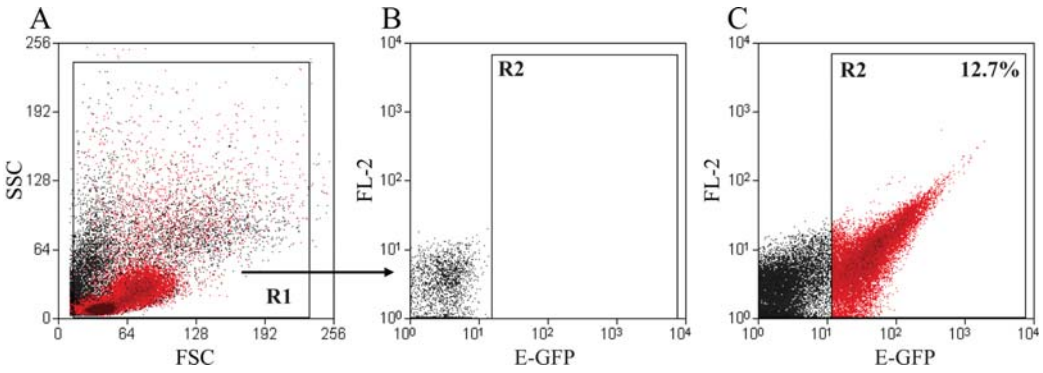

Figure 3. Re-sorting of VSELs from coculture with C2C12 cells. Morphology of cells derived from coculture, including C2C12 cells (marked in black) and E-GFP+ VSELs (marked in red), visualized by dot plots showing forward scatter (FSC) vs. side scatter (SSC) signals, related to the size and granularity/complexity of the cell, respectively (panel A). C2C12 cells derived from region R1 and which do not exhibit expression of E-GFP (panel B). Expression of E-GFP in whole population of cells derived from region R1. E-GFP+ VSELs are included in region R2 and are shown in red. Percentage shown is representative of the content of E-GFP+ VSELs in the analyzed coculture (panel C).

Table I. Sequence of primers for real-time RT-PCR.

Primer	Sequence
ß2-micro-globulin	5'-CAT ACG CCT GCA GAG TTA AGC A-3' 5'-GAT CAC ATG TCT CGA TCC CAG TAG-3'
Nkx2.5/Csx	5'-CGG ATG TGG CTC GTT TGC-3' 5'-TTG GGA CCC TCC CGA GAT-3'
GATA-4	5'-TCC AGT GCT GTC TGC TCT AAG C-3' 5'-TGG CCT GCG ATG TCT GAG T-3'
Troponin I	5'-TGC GAA ACC GGA TCA ATG A-3' 5'-CGC CCG GTG ACT TTG G-3'
Mybpc3	5'-TGA AGG GTC AGT CTC GGT AAC C-3' 5'-AGA AAG AGG CCA ATA GGG TCA TC-3'
Actn2	5'-TGA AGA AAT AGT CGA TGG CAA TGT-3' 5'-GCG AAG CGG AGG ATG ATG-3'
Actn3	5'-CTG GGC ATG ATC TGG ACC AT-3' 5'-TGG CTG AGG TCT CTT CTA CAG AGA-3'

In vitro expansion of VSELs. Fig. 2 illustrates the protocol of VSELs expansion utilized in this study. Freshly sorted VSELs were plated over a C2C12 murine myoblast feeder layer in DMEM media with 2% FBS at 37˚C in 5% CO_2. After 7 days of co-culture with C2C12 cells, approximately 5-10% of all VSELs form sphere-like clusters consisting of a few hundred cells resembling embryoid bodies (VSEL-derived spheres, VSEL-DSs). To verify their embryonic features, a sample of VSEL-DSs were fixed in 4% paraformaldehyde for 15 min, washed twice in TBST (20 mM Tris-HCl, pH 7.4, 0.15 M NaCl, 0.05% Tween-20) and cell stained for the expression of placenta-like alkaline phosphatase (PLAP) with Naphthol/Fast Red Violet (Chemicon, USA) for 15 min in room temperature. The number of positive, red-stained colonies was counted using an inverted microscope (Olympus America, Center Valley, PA) following final cell washing with TBST buffer. Unfixed VSEL-DSs were also trypsinized to obtain single cell suspensions which were resuspended in cell sorting medium and subsequently sorted by MoFlo to distinguish between the GFP+ VSELs and GFP- C2C12 myoblasts (Fig. 3).

Cardiomyogenic differentiation. EGFP+ VSELs ($5x10^4$) derived from VSEL-DSs, purified from co-culture system by FACS, were plated on culture dishes in DMEM with 10% heat-inactivated FBS, 4 mM L-glutamine, 4.5 g/l glucose and the following growth factors which were added every 24 h: 10 ng/ml basic FGF-2, 10 ng/ml VEGF and 10 ng/ml TGF-ß1 (R&D Systems, Inc.) (2). The cultures were examined after 20 days for the presence of troponin I by immunofluorescent staining and after 4, 6, 9, 12 and 16 days for the presence of early and mature cardiac markers by RQ-PCR.

Real-time RT-PCR (RTQ-PCR). Expression of cardiac markers (Nkx2.5/Csx, GATA-4, troponin I, Mybpc3, sarcomeric actinin 2, sarcomeric actinin 3) was measured. Total mRNA was isolated using RNeasy mini kit (Qiagen Inc., Valencia, CA, USA) and reverse-transcribed using TaqMan reverse transcription reagents (Applied Biosystems, Foster City, CA, USA). Measurements of mRNA levels of pluripotent and cardiac markers as well as ß2-microglobulin were performed by real-time RT-PCR using an ABI PRISM® 7000 sequence detection system (ABI, Foster City, CA, USA). The reaction mixture (25 μl) contained 12.5 μl SYBR-Green PCR Master Mix, 10 ng of cDNA template and appropriate primers (Table I). The primers were designed using Primer Express software. Threshold cycle (C_t), the cycle number at which the amount of the amplified gene of interest reached a fixed threshold, was subsequently determined. Relative quantification of marker gene mRNA expression was calculated by the comparative C_t method. The relative quantification value of the target gene, normalized to an endogenous control (ß2-microglobulin gene) and relative to a calibrator, was expressed as $2^{-\Delta\Delta Ct}$ (fold difference), where $\Delta_C = C_t$ of target genes, C_t of endogenous control gene (ß2-microglobulin); and $\Delta\Delta C_t = \Delta C_t$ of samples for target gene, ΔC_t of calibrator for the target gene. To avoid the possibility of amplifying contaminating DNA 1) all primers for real-time RT-PCR were designed with an intron sequence within the cDNA to

be amplified, 2) reactions were performed with appropriate negative controls (template-free controls), 3) the uniform amplification of the products was re-checked by analyzing the melting curves of the amplified products (dissociation graphs), 4) while the melting temperature (T_m) was 57-60˚C, the probe T_m was at least 10˚C higher than the primer T_m, and, finally, 5) gel electrophoresis was performed to confirm the correct size of the amplification and the absence of unspecific bands.

Immunofluorescent staining of VSELs. For immunofluorescent (IF) staining, VSELs were fixed in 3.5% paraformaldehyde for 20 min, permeabilized using 0.1% Triton X-100, washed in PBS, pre-blocked with 2% bovine serum albumin (BSA) and stained with anti-SSEA-1 (clone MC-480, 1:100, mouse monoclonal IgM; Chemicon, Temecula, CA) and Oct-4 (clone 9E3, 1:100, mouse monoclonal IgG1; Chemicon). Troponin I expression was evaluated after 20 days of EB-derived GFP+ VSELs differentiation. Cells were stained with anti-troponin I antibody (1:200, mouse monoclonal IgG2b; Chemicon). Appropriate secondary antibodies, Alexa Fluor 594 goat anti-mouse IgM and Alexa Fluor 594 goat anti-mouse IgG (1:400; Molecular Probes, Eugene, OR, USA) were used. Within the control experiments, cells were stained with secondary antibodies only. The nuclei were labeled with DAPI (Molecular Probes). Fluorescence images were acquired with the TE-FM Epi-Fluorescence system with Nikon Inverted Microscope Eclipse TE300 and HQ digital B/W CCD camera (Roper Scientific, Tucson, AZ, USA). The expression of each antigen was examined in cells from four independent sorts.

Preparation of cells for ImageStream system (ISS) analysis. Nucleated BM cells obtained after lysis of RBCs were washed twice in phosphate-buffered saline (PBS) and stained for the presence of Sca-1, CD45 and lineage markers (Lin) with the following rat anti-mouse antibodies (BD Pharmingen, San Jose, CA, USA): anti-CD45 (FITC; clone 30-F11), anti-Ly-6A/E (Sca-1) (PE-Cy5; clone E13-161.7) and anti-Lin markers including: anti-CD45R/B220 (PE; clone RA3-6B2), anti-Gr-1 (PE; clone RB6-8C5), anti-TCRαß (PE; clone H57-597), anti-TCRγδ (PE; clone GL3), anti-CD11b (PE; clone M1/70) and anti-Ter119 (PE; clone TER-119). Cells were subsequently fixed with 2% paraformaldehyde for 20 min in RT and permeabilized with 0.1% Triton X-100 for 10 min in RT. Nuclei were visualized following staining with 7-amino-actinomycin D (7-AAD) which was added 10 min before analysis (BD Pharmingen; 40 μM). For intranuclear staining against pluripotent marker Oct-4, freshly sorted VSELs were fixed with 2% paraformaldehyde for 20 min in RT, permeabilized with 0.1% Triton X-100 for 10 min in RT and subsequently stained with anti-mouse Oct-4 antibody (clone 9E3, 1:100, mouse monoclonal IgG1; Chemicon) followed by incubation with the secondary anti-mouse IgG antibody (FITC; BioLegend, San Diego, CA, USA). Cells were then re-stained with other directly conjugated antibodies against Sca-1 (PE-Cy5; clone E13-161.7), CD45 (PE; clone 30-F11) and Lin markers (PE). Nuclei were visualized with 7-AAD. All samples were analyzed with the ImageStream System 100 (Amnis Corporation, Seattle, WA, USA). Signals from FITC, PE, 7-AAD and PE-Cy5 were detected by channels 3, 4, 5 and 6, respectively, while side-scatter and brightfield images were collected by channels 1 and 2, respectively.

Table II. Scheme of the microarray experiment.

Exp. no.	Cy5	Cy3
1	VSELs	VSEL-DSs
2	Day 4	VSEL-DSs
3	Day 6	VSEL-DSs
4	Day 9	VSEL-DSs
5	Day 12	VSEL-DSs
6	Day 16	VSEL-DSs

Microarray analysis

Quality control and amplification of total RNA. Sample quality was checked using the Agilent 2100 Bioanalyzer platform (Agilent Technologies, Palo Alto, USA) and visualized by gel image and electropherogram using the Agilent 2100 Bioanalyzer software, generating an RNA integrity number (RIN). The RIN is calculated by a proprietary algorithm taking several QC parameters into account (e.g. 28S/18S peak area ratios, unexpected peaks in the 5S region). A RIN number of 10 indicates perfect RNA quality, a RIN number of 1 indicates bad RNA quality. Accordingly RNA with a RIN number >6 is of sufficient quality for gene expression profiling experiments (10). In our study, all RNA samples were found to have RIN values between 7.8 and 9.8. The linear T7-based amplification of the 1 μg RNA samples (4, 6, 9, 12 and 16 days VSEL-DSs) was performed. RNA yield from purified VSELs was not sufficient for the linear T7-based amplification and the SuperAmplification protocol (Miltenyi Biotec's proprietary protocol) was employed using 30 ng of the RNA samples from VSELs and VSEL-DSs. Isolation of mRNA was performed using magnetic bead technology. Amplified cDNAs were quantified using the ND-1000 Spectrophotometer (NanoDrop Technologies, Inc).

Hybridization and scanning of microarrays. Amplified samples were labeled with Cy3 and Cy5 according to the PIQOR™ protocol (Miltenyi Biotec's). The fluorescent-labeled probes were subsequently hybridized overnight on topic-defined PIQOR™ stem cell mouse antisense microarrays using a hybridization station (Table II). Hybridized PIQOR™ microarrays were scanned using the ScanArray™ Lite laser scanner (Perkin-Elmer Life Sciences, Boston, USA). Spots located in areas in which hybridization artifacts (e.g. air bubbles) occurred, were flagged and excluded for further analysis. Since each gene is spotted on 4 different positions on the array, even if one or two spots were flagged, sufficient replicates for valid data analysis still remained on the slide.

Image and data analysis. Mean signal and background intensities were obtained for each spot of the microarray images using the ImaGene software (Biodiscovery Inc., El Segundo, USA). Spots were analyzed using the PIQOR™ Analyzer software (Miltenyi Biotec GmbH, Bergisch Gladbach, Germany), automatically processing the raw data

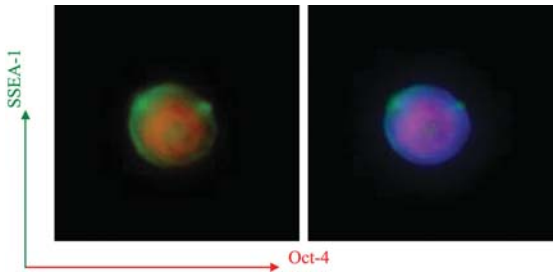

Figure 4. Immunofluorescent VSEL staining. Oct-4 staining is apparent in the nucleus and SSEA-1 expression in the cytoplasmic membrane.

derived from the ImaGene software (background subtraction, data normalization, calculation of Cy5/Cy3 ratios). As an additional quality filter, only those spots/genes for which, at least in one channel, the signal intensity >2 times the mean background were taken into account for the calculation of the Cy5/Cy3 ratio. The PIQOR™ Analyzer calculated all normalized mean Cy5/Cy3 ratios of the four replicates per gene. Genes that are >1.7-fold up- or downregulated represent putative candidate genes. Green indicates a <0.58-fold downregulation and red indicates a >1.7-fold induction of the respective gene in comparison to the control.

Statistical analysis. Data from RQ-PCR are reported as mean ± SD. All statistical analyses were performed using InStat (version 1.14, GraphPad, San Diego, CA, USA). Statistical significance was defined as P<0.01. The following steps of microarray analysis were performed: 1) overall comparison of expression profiles by global, inter-experiment correlation analysis, 2) masking of genes with too few (<4), or no expression values, and 3) categorization of the remaining genes into groups with different expression time courses. The self organizing tree algorithm was used, resulting in 11 different groups. For each of the 11 expression groups, genes were sub-classified in a hierarchical tree structure and pathway analysis was performed, with the aim to find biological pathways or other connections between the genes in any given coexpression group. The TreeRanker (Miltenyi Biotec) software was used to scan larger groups of genes and determine a common biological pathway affiliation and/or other commonalities. Furthermore, groups of genes were analyzed to determine statistically significant enrichments of biological pathways and related annotation terms. Term enrichment relative to the expected background distribution was scored using Fisher's exact test. Small numbers of putatively connected genes, i.e. those with good TreeRanker scores, were analyzed by the PathwayArchitect software (Stratagene). A molecular interaction database was scanned to retrieve up-to-date information on the biological interactions of the molecules of interest. In the database, information automatically extracted from PubMed is compiled by means of a text mining algorithm, extracting information on biological interactions from the scanned literature. PathwayArchitect supports a number of different analyses, searching for direct interactions between groups of input genes, or searching for common regulators or common targets of multiple genes contained in a query group (biological interaction network).

Results

Isolation and characterization of BM-derived VSELs. As shown in Fig. 1, VSEL population is very small and, in BM, represents ~0.03±0.01% of nucleated cells, approximately 10-times less than the population of hematopoietic stem cells (0.30±0.05%). VSELs express pluripotent stem cell markers Oct-4 and SSEA-1 as evidenced by immunofluorescent staining. Accordingly, transcription factor Oct-4 is expressed in the nuclei and antigen SSEA-1 on the cell surface (Fig. 4).

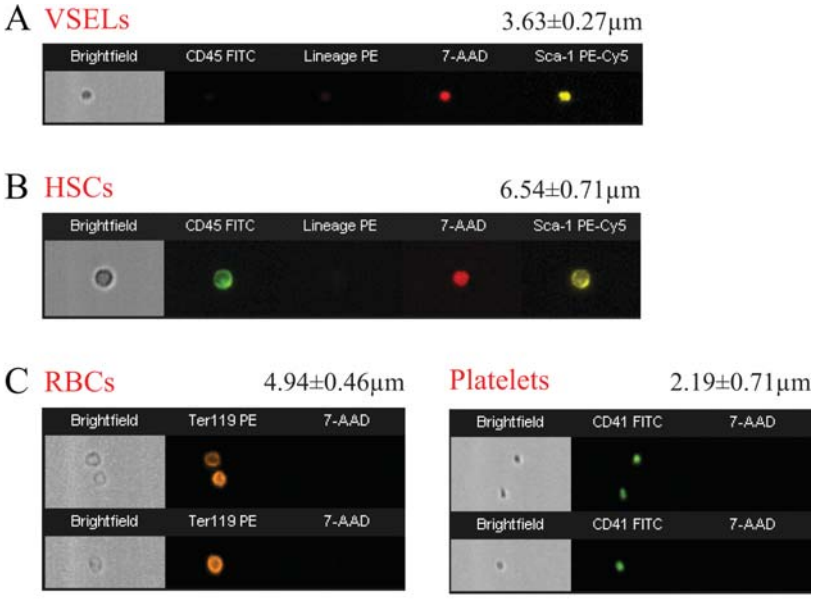

Figure 5. Morphological comparison of murine VSELs, HSCs, erythrocytes and platelets by ISS. Murine VSELs and HSCs are shown stained for CD45 (FITC, green), Lin (PE, orange) and Sca-1 (PE-Cy5, yellow), (panel A and B, respectively). Murine blood-derived erythrocytes and platelets stained for Ter119 (PE, orange) and CD41 (FITC, green), respectively, are shown (panel C). Following fixation, all samples were stained with 7-AAD (red) to visualize nuclei. Erythrocytes and platelets do not possess nuclei, while VSELs and HSCs show cellular structure containing nuclei. The average size of each population is shown (mean ± SD). All images are presented in the same magnification (scale bar = 10 μm).

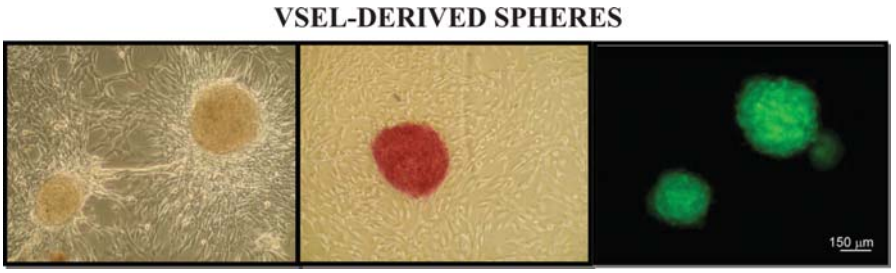

Figure 6. Staining of VSEL-DSs for fetal alkaline phosphatase. After 7 days of coculture, EGFP+ VSELs form sphere-like clusters consisting of a few hundred cells resembling embryoid bodies (VSEL-DSs) and expressing fetal alkaline phosphatase.

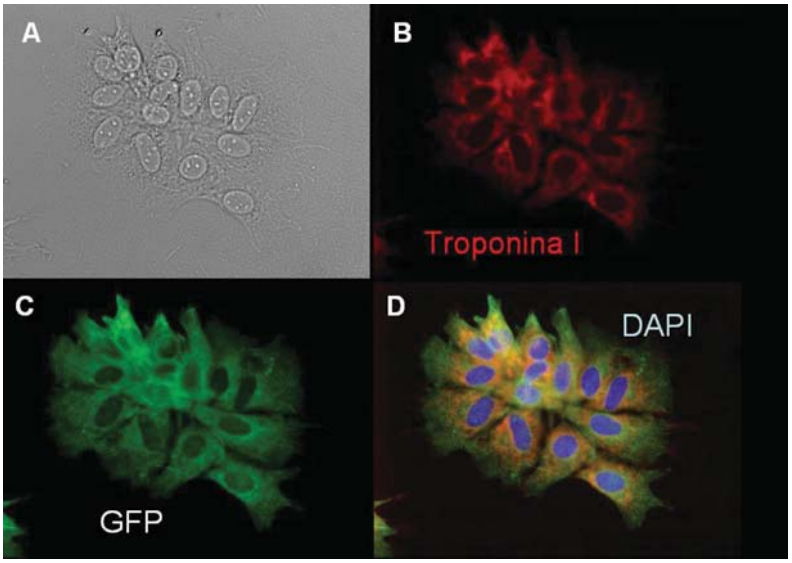

Figure 7. Immunofluorescent staining of VSEL-derived cardiomyocytes. Troponin I staining is shown in EGFP+ cardiomyocytes.

The further evaluation of freshly purified VSELs using ISS confirmed the presence of Oct-4 at the protein level and the colocalization thereof in fixed cells with DNA marker 7-AAD in nuclei and the presence of the Sca-1 antigen on cell surface. In agreement with FACS data, VSELs are lineage negative and do not express CD45 antigen (Lin^-CD45^-) (Fig. 5, panels A and B). Furthermore, the direct ISS-based comparison of BM-derived VSELs with other populations of BM-derived nucleated cells (monocytes, granulocytes) demonstrated that VSELs are small (3.63±0.27 μm) and smaller than hematopoietic stem cells (6.54±0.71 μm) and erythrocytes (4.94±0.46 μm). However, they are larger than platelets (2.19±0.71 μm) (panel C).

Two-step model for cardiomyogenic expansion/ differentiation of VSELs. We developed a two-step model for *ex vivo* expansion/differentiation of VSELs into cardiomyocytic lineages. In the first step, freshly sorted GFP^+ VSELs are plated over the feeder layer of C2C12 murine myoblasts where they form VSEL-DSs. Staining of VSEL-DSs for PLAP expression confirmed the embryonic phenotype of cells that compose these structures (Fig. 6).

In the next step, VSEL-DS are trypsinized and GFP^+ cells derived from the primary cultures are re-sorted from GFP^- C2C12 myoblasts and plated for 20 days into secondary cultures, where they ultimately become troponin I positive (Fig. 7). We measured expression of early cardiac markers in freshly isolated VSELs as well as cells derived from differentiating VSEL-DSs at day 4, 6, 9, 12 and 16 of expansion (Fig. 8). In comparison to BM mononuclear cells, freshly isolated VSELs were significantly enriched in mRNA for early cardiac transcription factors GATA-4 (~85-fold) and Nkx2.5/Csx (~50-fold). During differentiation, expression of GATA-4 and Nkx2.5/Csx decreased gradually, reaching levels 4- and 9-fold lower than in non-expanded VSELs. The expression of mRNA for troponin I was also significantly higher in VSELs than in MNCs, however it increased between 4 and 16 days of differentiation to levels 2-fold higher than in non-expanded VSELs. Levels of mRNA for Mybpc3, actinin 2 and actinin 3 increased gradually from 4 to 16 days to reach values 5- to 8-fold higher than in freshly sorted VSELs.

Gene expression profile. Gene expression profiles of differentiating VSELs had been measured after 4, 6, 9, 12 and 16 days of expansion. Gene candidates (727) with ≥4 valid measurements were subjected to a hierarchical tree analysis. We employed the self organizing tree algorithm (SOTA), which generates a defined number of categories and also specifies the relationship of these categories showing them in a tree-like structure. The master tree, demonstrating the

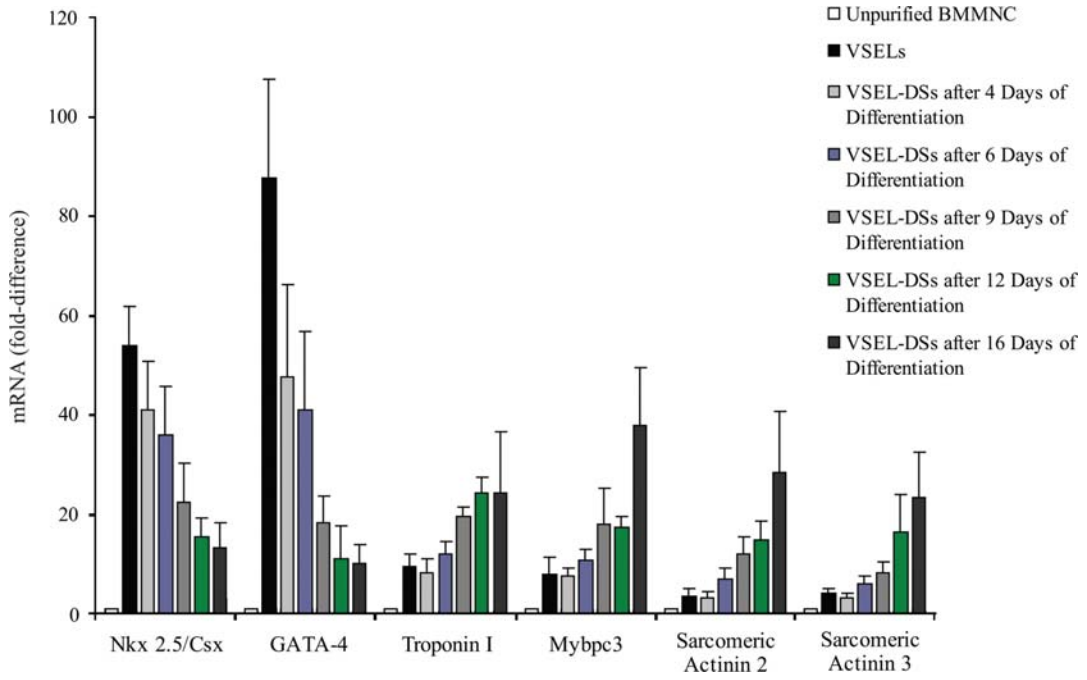

Figure 8. Gene expression profile during cardiac differentiation as measured by RTQ-PCR. Relative changes in expression of cardiac markers in BM-mononuclear cells, freshly purified VSELs and, after 4, 6, 9, 12 and 16 days of differentiation, VSEL-derived cardiomyocytes as measured by real-time RTQ-PCR. Expression of each gene is showed as a fold difference compared to ß2-microglobulin (control).

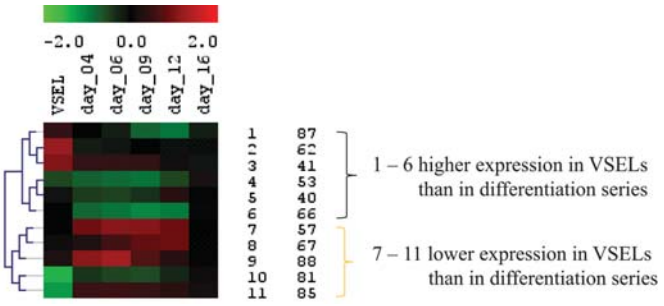

Figure 9. Gene expression profile master tree as measured by microarrays. Each horizontal line corresponds to single cluster of genes. Vertical lines correspond to time points of expression analysis (VSELs, after 4, 6, 9, 12 and 16 days of differentiation). Digits in the right column represent the cluster number and the number of genes included.

relationship between the clusters, is shown in Fig. 9. Each line corresponds to an entire cluster of genes. The first six clusters are characterized by a higher expression in VSELs, as compared to the differentiating cells. Among those, clusters 2 and 3 show a notable upregulation in VSELs (i.e. a stronger expression in VSELs than in VSEL-DSs), which disappears along the differentiation time. By contrast, clusters 4, 5 and 6 are characterized by similar levels of expression in VSELs and VSEL-DSs with subsequent downregulation during the differentiation period. The five remaining clusters 7-11 exhibit an opposite characteristic: gene expression was lower in VSELs than in the more differentiated cells. The similar clusters 10 and 11 contain genes that are downregulated in VSELs (i.e. lower in VSELs as compared to VSEL-DSs). These clusters have an opposite expression profile compared to those of clusters 2 and 3. Finally, clusters 7, 8 and 9 contain genes that are similarly expressed in VSELs and VSEL-DSs but are upregulated during the differentiation period. A detailed description of the gene expression profiles in clusters is shown in Table III.

Biological interaction networks (BINs). The previously described co-regulation group analysis highlighted the number of recurrent expression patterns within the dataset, some of which are of particular interest. One of the strongest effects observed was a rapid change in expression of some genes from the VSELs stage to the first differentiation time point. Several genes also showed an inverse expression pattern, i.e. they were upregulated in VSELs relative to VSEL-DSs but downregulated after 4 days, or vice versa.

In order to identify transcription factors or other regulators responsible for these effects, we employed a biological network analysis using PathwayArchitect software. Overall, the most frequently represented signalling pathways included TGF-ß, Wnt, FGF, BMP, chemoattractants and integrins. Several genes were identified which showed a particularly high expression in VSELs as compared to VSEL-DSs and which were then immediately lost or reversed during differentiation (early downregulation). Subsequently, the literature-mining component of PathwayArchitect was used to identify factors which have been described to regulate the expression of at least 2 genes in the query group. These regulatory factors included IFN-γ and TGF-ß which regulate 4 genes each. Similarly, group of genes with an early upregulation patterns (lower expression in VSELs than in VSEL-DSs) with subsequent rapid increase of expression early during differentiation was evaluated. TGF-ß regulated the expression of 14 different query genes; TNF and BMP6 regulated 9 and 7 genes, respectively.

Table III. Characterization of the gene expression profile in clusters of genes.[a]

Regulation pattern	Signalling pathway	Clusters/genes
Induction in VSELs	Chemokine receptor	Cluster 1: relative expression minimum after 9 and 12 days
Suppression during	Wnt/FZD	- CXCR4, PRKC, CD37
differentiation	TG-ß signalling	Cluster 2: higher expression in VSELs than in VSEL-DSs
	BMP signalling	- integrins α-4, α-IIB, ß-7
	Extracellular matrix regulators	- ITGA4, BGLAP, CD44, MMP9, AGC1, ITGB7, ITGA2B, CD47, COL11A2
	Integrin-mediated signalling	- ITGA4, CASP8, FGF8, TIE1, IHH, HAND1, PDGA, FGFR2, FKHR
	Angiogenesis	Cluster 3: upregulated in VSELs
		- CCNE1, HMGB2, ITGAL, MYL2, CCT8, CNP, CD44, ENG, FGFR4, HRAS, PLCE, DLX5, OB, RB, CLCN2
No regulation in VSELs	Angiogenesis	Cluster 4: strongest expression after 16 days
Suppression during	Chemoattractants	- VEGFD, tissue-type plasminogen activator, interleukin-6, thrombospondin-2,
differentiation	Transcription regulators	bone proteoglycan II, COL6A1, LAMA2 and LAMA4
	BMP signalling	Cluster 5: strongest expression after 12 days
	Extracellular matrix	- EN1, NGN3, OSF, RARA1, RARG1, RBL2, SMAD4, SNAI2, TBX5,
	Cell differentiation	TCF4, TFCOUP1
		Cluster 6: downregulation after 4-12 days
		- HGF
		- MMP21/22/23, NEUROD1, TGFBR1, HOXA2, PRKCE, PTCH2, TNNC1, PTEN1/2, NFKB2, EBCTF, NFATCB, plexin A3
		- TGFBR1, SMAD5, BMPR1B
		- COL12A1, COL9A3, COL4A1, MMP3, MMP1, MMP21/22/23
No regulation in VSELs	Ion channels	Cluster 7: expression highest after 4-12 days and lower in VSELs after 16 days
Induction during	BMP signalling	- CDK1, BUB1, BUB1B, THBS1, UBE2T, ITGA6, MAD2L1, SET,
differentiation		SEMA3A, CLF-1, PAK1, BMP7, CLCN6, KIAA0152, PRRX1, GABRA1,
	Growth factors	SEMA6A1
	Mitotic spindle-checkpoint	- CKD1, WEE1, BUB1, BUB1B, PCNA, KI67
	Mitotic exit network	Cluster 8: strong expression peak after 9 and 12 days
		- GJB4, COL1A1, COL1A2, LAMB3, DPYSL3, POU3F2, HGFR, LERK-5, COL5A2, S100A11, CD34, CRIP1, c-Met, Oct-7
		Cluster 9: expression peak after 4 and 6 days
		- FGF1, FGF4, FGF6, NGFB, WISP3, INHBA
		- BMP-4
		- K^+ channels (KCNA4, KCNH2, KCNJ3, KCNH5, KCNE3, KCNJ4, KCNJ5, KCNJ10, KCNJ11, KCNQ4)
		- $Ca2^+$ channels (CACNA1A, CACNA1C, CACNA1H)
		- Na^+ channel (SCN5A)
Supression in VSELs	Extracellular matrix regulators	Cluster 10: lowest expression in VSELs
Induction during	Angiogenesis	- EGF receptor (EGFR), fibroblast growth factor 7 (FGF7), MMP 2, nidogen
differentiation	Cardiac development	Cluster 11: downregulated in VSELs
	Cellular motility	- angiopoietin, VEGFα, VEGFC, Notch, sonic hedgehog
	Fibronectin receptor complex	- integrin ß-1, connexin-43, neuropilins NRP1 and NRP2, secreted factor sonic hedgehog, transcription factor POUF6F1, Notch, BMP-receptor 1

[a]Regulation patterns for two major groups of clusters (cluster 1-6 and 7-11) are characterized in the left column and the description of gene expression profiles for each of the 11 clusters including exemplary genes is described in the right column. The middle column contains the functional annotation of significantly regulated genes into signalling or metabolic pathways.

Discussion

In the present study we demonstrated that pure VSELs can be effectively isolated from murine BM and subsequently expanded into cardiac myocytes in a two-step *ex vivo* expansion model. Differentiation of VSELs into VSELs-DSs and, subsequently, into cells from VSELs-DSs and cells into cardiomyocytes was evaluated using RTQ-PCR, microarrays and epifluorescence staining.

BM-derived VSELs are a rare subpopulation (~0.01%) of non-hematopoietic Sca-1$^+$, Lin$^-$, CD45$^-$ cells that express markers of PSCs (e.g., Oct-4, Nanog and SSEA-1). Electron microscopy and ISS demonstrated that VSELs have a relatively large nucleus containing open-type chromatin and their morphology resemble embryonic stem cells (ESC).

In cocultures with C2C12 myoblasts, approximately 7-10% of purified VSELs form spheres resembling fetal alkaline phosphatase positive embryoid bodies. Cells derived from VSEL-DSs after replating into tissue specific differentiation media have the capability of differentiation into all three germ layers, including mesoderm-derived cardiac myocytes (2,5).

Several types of stem and progenitor cells are reported to be capable of cardiomyogenic differentiation, including BM-derived cells (HSCs, MSCs, MAPCs), resident cardiac stem cells (side population, c-kit$^+$, Isl-1$^+$), blood or tissue-derived cells (adipose tissue stem cells, EPCs) and, most recently, PSCs (ESCs, iPSCs) (11). A study recently published by Pallante *et al* demonstrated the potential cardiomyogenic capability of a population of BM-derived Oct3/4$^+$c-kit$^+$ cells in adult mice. These cells were, like VSELs, non-hematopoietic (CD45$^-$) and expressed CXCR4, but, in contrast to VSELs, do not express Sca-1 antigen. However, in response to PDGF they gave rise to cardiac myocytes expressing ß-adrenergic receptors, cardiac proteins (troponin T, α-sarcomeric actinin, α-cardiac actin, α- ß-MHC, connexin 43 and 40) that show spontaneous chronotropic activity. Chronotropic activity was modulated by ß-agonist isoproterenol. Troponin T$^+$ cells started to form at the periphery of cell clusters after 7 days and chronotropic activity was observed after 14 days of differentiation. Importantly, efficiency of cardiac differentiation of Oct3/4$^+$ cells declined with age (12). The differentiation pattern of BM-derived cardiomyocytes was similar to that observed in embryonic cell-derived cardiomyocytes (12,13). Pallante *et al* confirmed that the cardiogenic Oct3/4$^+$ cells were rare (0.05%) within BM cells localized in the osteoblastic niche. Importantly, these cells are non-hematopoietic, negative for MSC markers and express CXCR4, indicating that they may correspond with VSELs (12).

Using RTQ-PCR and microarrays, our study suggests that VSEL differentiation follows the same pattern of gene expression changes as the differentiation of CMs during embryogenesis (14). RTQ-PCR revealed a gradually decreased expression of early cardiac markers (GATA-4, Nkx2.5/Csx) with a concomitant increase of the expression of genes encoding for cardiac proteins (troponin, actinin) during differentiation. Microarray results suggest typical early induction of several pivotal regulators of cardiac differentiation (Wnt, TGF-ß, BMP, FGF) with their gradual suppression during differentiation. The cardiogenic potential of VSELs is probably relevant to myocardial repair, due to their rapid mobilization in response to myocardial ischemia during acute MI. In mice, the mobilized cells are mRNA enriched for cardiac and endothelial markers. Recently, we showed that in patients with MI, the number of circulating VSELs increases as soon as 12 h after the onset of symptoms and that circulating human VSELs are significantly mRNA enriched for cardiac lineage (GATA-4, Nkx2.5/Csx, MEF2C) and endothelial (VE-cadherin) markers (4,9). Our data suggest that patients with MI who sustained larger myocardial injury have reduced VSEL mobilization (9,15). In mice, injection of G-CSF induced rapid mobilization of VSELs with upregulation of genes encoding for early developmental markers. Level of expression of PSC markers in VSELs is comparable to murine embryonic cell line ES-D3. Importantly, VSELs mobilized by G-CSF are capable of differentiation into mesoderm-derived cardiomyocytes, endoderm-derived pancreatic cells and ectoderm-derived neurons (16). Also, the number of circulating VSELs is reduced in older mice, corresponding to lower expression of PSC markers in blood and BM-derived VSELs (16). We hypothesized that the mobilization of VSELs observed in mouse models of tissue injury, and also in patients with MI and stroke, is a reparative mechanism to replenish the pool of local tissue-resident stem cells, such as cardiac stem cells (17). Indirect evidence that VSELs may contribute to cardiac repair and undergo differentiation into cardiac structures was shown by Dawn *et al* by employing an MI model in which mice underwent coronary occlusion and 48 h later received direct intramyocardial injection of VSELs or HSCs. Treatment with VSELs lead to improved contractility and reduced remodeling as well as reduced myocyte hypertrophy after 35 days of follow-up. No such benefits were observed in mice receiving HSCs. Interestingly, some, though rare, VSEL-derived GFP$^+$ cardiac myocytes were found to be present in the recipients' myocardia (8). However, it should be noted that VSELs used in the study were not expanded on the feeder layer, did not undergo clustering into ES-DS, nor were differentiated towards cardiac lineage prior to injection. A study recently reported by Ceselli *et al* demonstrated the presence of populations of multipotent progenitor cells (MPCs) expressing PSC markers (Oct 3/4, Nanog, Sox2, c-Myc, Klf4) in human BM and peripheral blood. MPCs were shown to be self-renewing, clonogenic and multipotent, including the ability to differentiate into cardiac myocytes. MPC-derived cardiomyocytes were positive for connexin 43 and displayed spontaneous intracellular calcium movement. Microarray analysis revealed embryonic marker enrichment of MPCs. The phenotype of MPCs is more immature than MSCs, although both types of cells express similar surface markers (18).

Several groups obtained *in vitro*, spontaneously beating, early CMs from human ESCs (19-21). However, only limited groups of genes were assayed during differentiation. Synnergren *et al* used microarrays to assess the global expression profile of human ESC-derived CMs and demonstrated that such cardiac cells have 530 upregulated and 40 downregulated genes. This genetic profile of ESC-derived CMs resembles normal human cardiac cells. Several early and late cardiac commitment markers were significantly

upregulated in ESC-derived CMs (TBX5, MEF2C, GATA-4, ISL1, TnT, MYH6). Importantly, these findings are in agreement with data obtained from analysis of human fetal CMs (22,23). Similar to our findings, the authors demonstrated that differentiated CMs display downregulation of PSC markers (Oct-4, Nanog, Sox2) in comparison to ESCs, which is biologically plausible. Also, we showed that MYH, which is a promoter of human ESC-derived CM differentiation, is also induced in VSELs-derived CMs (23). Upregulated genes in VSELs-derived CMs show similar functional annotations as those in human ESC-derived CMs, such as calcium channels, cardiac and vascular development and cell differentiation (24). In our study, the generation of biological interactions networks (BIN) was attempted to identify factors which have been previously described to regulate multiple genes. Among the regulatory factors identified in several groups of genes showing similar behavior (early downregulation, early upregulation, regulation during differentiation, fibronectin receptor complex), TGF-ß, TNF and BMP6 were identified. Temporal changes in the transcriptional profile of differentiating human ESC-derived CMs were investigated by Beqqali *et al*. They showed that during differentiation of human ESCs, patterns of gene expression with early upregulation of embryonic genes followed by induction of mesoderm-specific and cardiac-specific genes occurred (25).

In addition to murine and human ESCs, multipotent cells, such as BM-derived MSCs, were shown in several studies to differentiate into cardiomyocytes (26). Using different stimuli (5-aza-deoxycytidine; insulin with dexamethasone and ascorbic acid) spontaneously beating cells expressed cardiac markers (ANP, MLC2a, GATA-4, NkX2.5) (11).

Several aspects of VSEL isolation need consideration. Isolation was carried out using the FACS-based live cell sorting protocol which was developed by our group. It validated the inclusion of small events (2-6 μm) in the sorting of events contained in extended lymphate using synthetic beads of defined size. Also, nucleated cells were isolated by lysis of erythrocytes instead of using the Ficoll-based protocol as the latter might have led to the losing of very small cells (27). Use of ISS allowed the integration of data derived from FACS and immunofluorescence including information on the colocalization of multiple cellular markers. In our study, VSELs stained positive for nuclear transcription factor Oct-4 and cell surface marker SSEA-1. VSELs are ~3-4 μm and are significantly smaller than HSCs and comparable in size to red blood cells (27).

Pluripotent stem cells, including VSELs, seem to be an optimal source of cells for studies on cardiac repair as they can be efficiently isolated from adult BM, expanded in culture and differentiated. Importantly, it seems that the process of their cardiogenic differentiation follows the same pattern as do embryonic stem cells. We postulate that human VSELs are promising cells for utilization in future clinical studies of patients with ischemic cardiomyopathy. However, their cardiogenic potential should be confirmed in humans and technical issues regarding their isolation, expansion and differentiation need to be addressed. The present study supports the hypothesis that murine BM-derived VSELs expressing PSCs and early cardiac-lineage markers can be efficiently expanded *in vitro* and differentiated into cardiac myocytes.

Acknowledgements

The work was supported by grants of the National Institutes of Health (R01 CA106281-01), Servier research grant and European Union structural funds, Innovative Economy Operational Programme, grant no. POIG 01.02-00-109/09 'Innovative methods of stem cells applications in medicine' and Polish Ministry of Science and Higher Education grants 0651/P01/2007/32, 2422/P01/2007/32.

References

1. Wollert KC and Drexler H: Cell-based therapy for heart failure. Curr Opin Cardiol 21: 234-239, 2006.
2. Kucia M, Reca R, Campbell FR, *et al*: A population of very small embryonic-like (VSEL) CXCR4(+)SSEA-1(+)Oct-4+ stem cells identified in adult bone marrow. Leukemia 20: 857-869, 2006.
3. Ratajczak MZ, Kucia M, Ratajczak J and Zuba-Surma EK: A multi-instrumental approach to identify and purify very small embryonic like stem cells (VSELs) from adult tissues. Micron 40: 386-393, 2009.
4. Kucia M, Dawn B, Hunt G, *et al*: Cells expressing early cardiac markers reside in the bone marrow and are mobilized into the peripheral blood after myocardial infarction. Circ Res 95: 1191-1199, 2004.
5. Ratajczak MZ, Zuba-Surma EK, Machalinski B, Ratajczak J and Kucia M: Very small embryonic-like (VSEL) stem cells: purification from adult organs, characterization, and biological significance. Stem Cell Rev 4: 89-99, 2008.
6. Ratajczak MZ, Machalinski B, Wojakowski W, Ratajczak J and Kucia M: A hypothesis for an embryonic origin of pluripotent Oct-4(+) stem cells in adult bone marrow and other tissues. Leukemia 21: 860-867, 2007.
7. Kucia M, Halasa M, Wysoczynski M, *et al*: Morphological and molecular characterization of novel population of CXCR4$^+$ SSEA-4$^+$ Oct-4$^+$ very small embryonic-like cells purified from human cord blood: preliminary report. Leukemia 21: 297-303, 2007.
8. Dawn B, Tiwari S, Kucia MJ, *et al*: Transplantation of bone marrow-derived very small embryonic-like stem cells attenuates left ventricular dysfunction and remodeling after myocardial infarction. Stem Cells 26: 1646-1655, 2008.
9. Wojakowski W, Tendera M, Kucia M, *et al*: Mobilization of bone marrow-derived Oct-4$^+$ SSEA$^-$4$^+$ very small embryonic-like stem cells in patients with acute myocardial infarction. J Am Coll Cardiol 53: 1-9, 2009.
10. Fleige S and Pfaffl MW: RNA integrity and the effect on the real-time qRT-PCR performance. Mol Aspects Med 27: 126-139, 2006.
11. Reinecke H, Minami E, Zhu WZ and Laflamme MA: Cardiogenic differentiation and transdifferentiation of progenitor cells. Circ Res 103: 1058-1071, 2008.
12. Pallante BA, Duignan I, Okin D, *et al*: Bone marrow Oct3/4$^+$ cells differentiate into cardiac myocytes via age-dependent paracrine mechanisms. Circ Res 100: E1-E11, 2007.
13. Laflamme MA, Gold J, Xu C, *et al*: Formation of human myocardium in the rat heart from human embryonic stem cells. Am J Pathol 167: 663-671, 2005.
14. Zaffran S and Frasch M: Early signals in cardiac development. Circ Res 91: 457-469, 2002.
15. Wojakowski W, Tendera M, Zebzda A, *et al*: Mobilization of CD34(+), CD117(+), CXCR4(+), c-met(+) stem cells is correlated with left ventricular ejection fraction and plasma NT-proBNP levels in patients with acute myocardial infarction. Eur Heart J 27: 283-289, 2006.
16. Kucia MJ, Wysoczynski M, Wu W, Zuba-Surma EK, Ratajczak J and Ratajczak MZ: Evidence that very small embryonic-like stem cells are mobilized into peripheral blood. Stem Cells 26: 2083-2092, 2008.
17. Wojakowski W, Kucia M, Kazmierski M, Ratajczak MZ and Tendera M: Circulating progenitor cells in stable coronary heart disease and acute coronary syndromes: relevant reparatory mechanism? Heart 94: 27-33, 2008.
18. Cesselli D, Beltrami AP, Rigo S, *et al*: Multipotent progenitor cells are present in human peripheral blood. Circ Res 104: 1225-1234, 2009.

19. Lev S, Kehat I and Gepstein L: Differentiation pathways in human embryonic stem cell-derived cardiomyocytes. Ann NY Acad Sci 1047: 50-65, 2005.
20. Kehat I, Kenyagin-Karsenti D, Snir M, *et al*: Human embryonic stem cells can differentiate into myocytes with structural and functional properties of cardiomyocytes. J Clin Invest 108: 407-414, 2001.
21. Xu C, Police S, Hassanipour M and Gold JD: Cardiac bodies: a novel culture method for enrichment of cardiomyocytes derived from human embryonic stem cells. Stem Cells Dev 15: 631-639, 2006.
22. Synnergren J, Akesson K, Dahlenborg K, *et al*: Molecular signature of cardiomyocyte clusters derived from human embryonic stem cells. Stem Cells 26: 1831-1840, 2008.
23. Beqqali A, Kloots J, Ward-van Oostwaard D, Mummery C and Passier R: Genome-wide transcriptional profiling of human embryonic stem cells differentiating to cardiomyocytes. Stem Cells 24: 1956-1967, 2006.
24. Synnergren J, Adak S, Englund MC, *et al*: Cardiomyogenic gene expression profiling of differentiating human embryonic stem cells. J Biotechnol 134: 162-170, 2008.
25. Beqqali A, van Eldik W, Mummery C and Passier R: Human stem cells as a model for cardiac differentiation and disease. Cell Mol Life Sci 66: 800-813, 2009.
26. Chugh AR, Zuba-Surma EK and Dawn B: Bone marrow-derived mesenchymal stems cells and cardiac repair. Minerva Cardioangiol 57: 185-202, 2009.
27. Zuba-Surma EK, Kucia M, Abdel-Latif A, *et al*: Morphological characterization of very small embryonic-like stem cells (VSELs) by ImageStream system analysis. J Cell Mol Med 12: 292-303, 2008.